AFRL-AFOSR-UK-TR-2012-0028

Asymptotic Description of Damping Mistuning Effects on the Forced Response of Turbomachinery Bladed Disks

Professor Carlos Martel

Universidad Politecnica de Madrid
Depto. Fundamentos Matematicos
E.T.S.I. Aeronauticos
Plaza Cardenal Csineros 3
Madrid, Spain 28040

EOARD Grant 11-3084

Report Date: July 2012

Final Report from 23 August 2011 to 22 August 2012

Air Force Research Laboratory
Air Force Office of Scientific Research
European Office of Aerospace Research and Development
Unit 4515 Box 14, APO AE 09421

REPORT DOCUMENTATION PAGE

Form Approved OMB No. 0704-0188

1. REPORT DATE *(DD-MM-YYYY)*	2. REPORT TYPE	3. DATES COVERED *(From – To)*
31 July 2012	Final Report	23 August 2011 – 22 August 2012

4. TITLE AND SUBTITLE

Asymptotic Description of Damping Mistuning Effects on the Forced Response of Turbomachinery Bladed Disks

5a. CONTRACT NUMBER

FA8655-11-1-3084

5b. GRANT NUMBER

Grant 11-3084

5c. PROGRAM ELEMENT NUMBER

61102F

6. AUTHOR(S)

Professor Carlos Martel

5d. PROJECT NUMBER

5d. TASK NUMBER

5e. WORK UNIT NUMBER

7. PERFORMING ORGANIZATION NAME(S) AND ADDRESS(ES)

Universidad Politecnica de Madrid
Depto. Fundamentos Matematicos
E.T.S.I. Aeronauticos
Plaza Cardenal Csineros 3
Madrid, Spain 28040

8. PERFORMING ORGANIZATION REPORT NUMBER

N/A

9. SPONSORING/MONITORING AGENCY NAME(S) AND ADDRESS(ES)

EOARD
Unit 4515 BOX 14
APO AE 09421

10. SPONSOR/MONITOR'S ACRONYM(S)

AFRL/AFOSR/RSW (EOARD)

11. SPONSOR/MONITOR'S REPORT NUMBER(S)

AFRL-AFOSR-UK-TR-2012-0028

12. DISTRIBUTION/AVAILABILITY STATEMENT

Approved for public release; distribution is unlimited. (approval given by local Public Affairs Office)

13. SUPPLEMENTARY NOTES

14. ABSTRACT

This is the final report of the research grant FA8655-11-1-3084 issued by the European Office of Aerospace Research and Development. This research effort is devoted to the analysis of the effect of damping mistuning on the forced response of turbomachinery bladed disks using asymptotic techniques. In particular it includes: (i) the derivation of the simplified Asymptotic Mistuning Model (AMM) for the general problem of the forced response of a bladed disk with damping mistuning, starting from the full general FE model description of the vibration of the rotor, (ii) the analysis of the most frequent situations of forcing (iia) isolated, disk dominated modes and (iib) clustered, blade dominated modes, and (iii) the checking of the AMM predictions against the results form a 1 DOF per sector mass-spring system, and the computation, for both forcing cases, of the damping mistuning pattern that produces the maximum amplification of the vibration.

15. SUBJECT TERMS

EOARD, Turbomachinery

16. SECURITY CLASSIFICATION OF:			17. LIMITATION OF ABSTRACT	18, NUMBER OF PAGES	19a. NAME OF RESPONSIBLE PERSON
a. REPORT	b. ABSTRACT	c. THIS PAGE			Gregg Abate
UNCLAS	UNCLAS	UNCLAS	SAR	44	19b. TELEPHONE NUMBER *(Include area code)* +44 (0)1895 616021

Asymptotic description of damping mistuning effects on the forced response of turbomachinery bladed disks

July 31, 2012

Final report to the European Office of Aerospace Research and Development
Research grant: FA8655-11-1-3084

Carlos Martel (carlos.martel@upm.es)
Depto. Fundamentos Matemáticos
E.T.S.I. Aeronáuticos
Universidad Politécnica de Madrid
28040 Madrid, SPAIN

Table of Contents

List of Figures

Summary

This is the final report of the research grant FA8655-11-1-3084 issued by the European Office of Aerospace Research and Development. This research effort is devoted to the analysis of the effect of damping mistuning on the forced response of turbomachinery bladed disks using asymptotic techniques. In particular it includes: (i) the derivation of the simplified Asymptotic Mistuning Model (AMM) for the general problem of the forced response of a bladed disk with damping mistuning, starting from the full general FE model description of the vibration of the rotor, (ii) the analysis of the most frequent situations of forcing (iia) isolated, disk dominated modes and (iib) clustered, blade dominated modes, and (iii) the checking of the AMM predictions against the results form a 1 DOF per sector mass-spring system, and the computation, for both forcing cases, of the damping mistuning pattern that produces the maximum amplification of the vibration.

Introduction

The term mistuning refers to the small differences among the (theoretically perfectly identical) blades in real turbomachinery bladed disk. These small undesirable random imperfections result from manufacturing, assembling and material tolerances, as well as in-service wear, and are essentially unavoidable.

Mistuning strongly influences the dynamical response of the bladed disk and, in particular, it typically leads to a considerable amplification of the vibration amplitudes of individual blades, which can significantly exceed the corresponding forced responses of the tuned (i.e., without imperfections) structure. These increased response levels result in a higher risk of High Cycle Fatigue (HCF) failures, with the corresponding strong negative impact on the safety, operability and readiness of aircraft turboengines.

According to the 1998 study of the HCF Science and Technology program [**?**], HCF was estimated to be responsible for the 56% of all Class A mishaps (a Class A mishap is one that results in over $1.000.000 in damage, loss of aircraft, loss of a life or permanent total disability), and 30% of all jet engine maintenance costs. It is, therefore, of great interest to work towards understanding the action mechanisms of mistuning, in order to try to devise ways to reduce or limit its amplification effect on the vibration amplitude.

The mistuning effect on bladed disks vibration have been extensively studied since the 70's (see, e.g., the reviews by Slater et al. [1] and by Castanier and Pierre [2], and the more recent presentation by Ewins [3]), and it still continues to be a topic of active research (in the recent ASME Turbo Expo 2011 Conference there were several mistuning related sessions). The well known main conclusions about the consequences of mistuning can be briefly summarized as follows: (i) mistuning can give rise to a large increase of the forced response vibration levels, and (ii) mistuning has a stabilizing effect on the aeroelastic instabilities, that is, it tends to reduce flutter induced vibrations.

The above mistuning results correspond to small variations of the elastic characteristics (mass and stiffness) of the blades, which is the situation considered in the vast majority of mistuning studies. In this research work, it is analyzed the not so frequent case of damping mistuning, where the bladed disk exhibits a blade to blade

variation of the damping.

Damping variation is always present in realistic situations, and it is typically due to the scatter present in material damping values, and also to the large variability of the damping produced at friction and interface joints. For example, in the case of the turbine wheels produced for turbochargers for the automotive industry, a blade damping variation of 30% or more is not unusual [4]. Also, for integrally bladed rotors, damping variation can be related to the application of damping coatings. The thickness of the film controls the resulting damping, and small errors in the coating thickness produce large variations of the damping. In both cases the resulting blade to blade damping variations are large, and the existing analysis [5, 6, 7] indicate that the vibration amplification is comparable to that produced by elastic mistuning.

Lin and Mignolet [5] statistically analyzed the effect of damping mistuning on the forced response of bladed disks using a simplified 1 DOF per sector model, and they concluded that damping mistuning can lead to variations in the blade vibration amplitude similar to that found with mass/stiffness mistuning. In the more recent work of Siewert and Stüer [6] a Reduced Order Model (ROM) derived from a complete bladed disk with damping mistuning is analyzed. The results from the ROM are first successfully compared with those from a detailed FEM simulation of the forced response of the mistuned rotor, and then the ROM is used to statistically analyze the effect of damping mistuning. They confirm that the magnitude of the resulting amplification factors is comparable to those from mass/stiffness mistuning, but the required damping mistuning levels are much higher. Also, from the figures in their paper, it can be clearly appreciated the interesting fact that damping mistuning does not produce any noticeable frequency splitting. A more elaborated mistuned ROM is developed in [7], which includes blade alone modes and takes into account the motion of the disk-blade interface. This ROM is then applied to statistically explore the mistuning patterns in order to obtain the maximum possible amplification for different engine order excitations, and, as in the previous case, large amplifications factors are found that require large damping mistuning levels, up to %80 of the damping average.

The analyses available in the literature mostly perform statistical explorations on reduced order models to get information about the vibration amplification levels due to damping mistuning. The purpose of this research effort is to apply asymptotic

techniques to derive a simplified Asymptotic Mistuning Model (AMM), which gives quantitatively accurate results and, what is more important, allows to identify the physical mechanisms that play a role in the effect of damping mistuning.

The AMM can be regarded as an extension of the Fundamental Mistuning Model (FMM) [8, 9, 10] for the very frequent situations in which all modes of the family do not share the same frequency (see CM and IM in Fig. 1). The derivation of the AMM is performed using a fully consistent asymptotic expansion procedure on the complete mistuned bladed disk model, and it does not require to select and assemble the blade alone and disk modes as in the Component Mode Synthesis (CMS) procedure. The AMM has been already used for the study of the optimal intentional (mass/stiffness) mistuning patterns for the stabilization of aerodynamically unstable rotors [11], and for the analysis of the forced response mistuning amplification [12], and its accuracy has been successfully checked against high fidelity FEM simulations [13, 14].

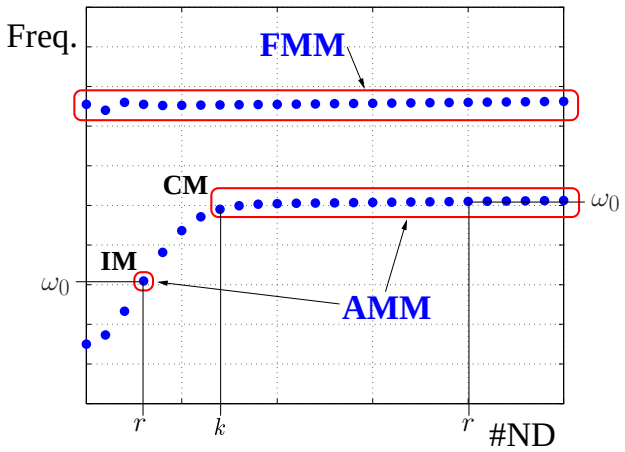

Figure 1: Sketch of tuned natural vibration frequencies vs. number of nodal diameters for a bladed-disk. The FMM applies only to the forcing of a modal family with very similar frequencies. The AMM can describe also the forcing of other modal configurations, like isolated modes (IM) and clustered modes (CM).

This research work is organized as follows. In the first part (Methods, Assumptions, and Procedures), a detailed derivation of the Asymptotic Mistuning Model (AMM) for the general problem of the forced vibrational response of a bladed disk with damping mistuning is performed. The second part (Results and Discussion) presents, in the first section, the application of the AMM to the description of the

effect of damping mistuning on the forcing of two isolated modes (IM in Fig. 1). In the second section, the AMM is applied to describe the forcing of a mode that belongs to a cluster of modes with nearly equal tuned vibration frequency (CM in Fig. 1). In both cases the mistuning pattern that gives maximum amplification of the vibration amplitude is computed, and the AMM results are quantitatively checked against those from a 1 DOF per sector mass-spring model. Finally, a summary of the obtained results together with some concluding remarks are drawn in the last part (Conclusions).

Methods, Assumptions, and Procedures

Forced response of a bladed disk with damping mistuning

In this section, the problem of the forced response of a general bladed disk with damping mistuning is considered, and it is expressed in the tuned TW basis to simplify the derivation process of the AMM.

The starting point is the equations of motion of the full FEM discretization of the forced bladed disk,

$$\mathbf{K} \cdot x + \mathbf{M} \cdot \ddot{x} = f(t), \tag{1}$$

where x and f are, respectively, the displacement of the independent DOF, and the forcing vector. The tuned bladed disk is a cyclic structure, that is, it is made of a sector that is repeated N times in the circumferential section to complete the structure (see Fig. 2).

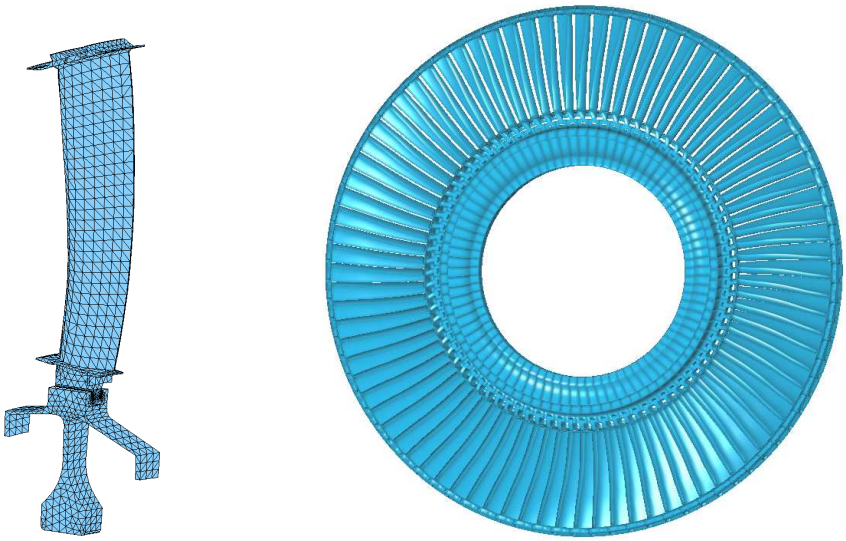

Figure 2: Left: detail of the sector of a sample turbomachinery rotor. Right: complete bladed disk.

It is assumed that the forcing takes the form of a traveling wave excitation with frequency ω and engine order r,

$$f(t) = \mathbf{F}\mathrm{e}^{\mathrm{i}\omega t} + \text{c.c.},$$

where c.c. stands for the complex conjugate. The response, consequently, can be written as a complex mode shape $\mathbf{X}$ with frequency ω,

$$x(t) = \mathbf{X}\mathrm{e}^{\mathrm{i}\omega t} + \text{c.c.},$$

which is given by the following linear, time independent system

$$\left[\mathbf{K} - \omega^2 \cdot \mathbf{M}\right] \cdot \mathbf{X} = \mathbf{F}.$$

The mass $\mathbf{M}$ and stiffness $\mathbf{K}$ matrices are cyclic symmetric matrices

$$\mathbf{K} = \begin{bmatrix} K & K_c & 0 & \cdots & K_c^T \\ K_c^T & K & K_c & & 0 \\ 0 & \ddots & \ddots & \ddots & \vdots \\ \vdots & & \ddots & \ddots & \vdots \\ K_c & 0 & \cdots & K_c^T & K \end{bmatrix}, \; \mathbf{M} = \begin{bmatrix} M & M_c & 0 & \cdots & M_c^T \\ M_c^T & M & M_c & & 0 \\ 0 & \ddots & \ddots & \ddots & \vdots \\ \vdots & & \ddots & \ddots & \vdots \\ M_c & 0 & \cdots & M_c^T & M \end{bmatrix}, \tag{2}$$

and the forcing term can be expressed as,

$$\mathbf{F} = \begin{bmatrix} Fe^{i(2\pi r/N)1} \\ \vdots \\ Fe^{i(2\pi r/N)j} \\ \vdots \\ Fe^{i(2\pi r/N)N} \end{bmatrix},$$

once the vector $\mathbf{X}$ is arranged by sectors

$$\mathbf{X} = \begin{bmatrix} X_1 \\ \vdots \\ X_j \\ \vdots \\ X_N \end{bmatrix},$$

with the vector X_j containing the displacements of the m DOF associated with sector j.

In order to take into account the sector to sector mistuning damping in our model,

a damping matrix $\mathbf{C}$ is included

$$\left[\mathbf{K} + \mathrm{i}\mathbf{C} - \omega^2 \cdot \mathbf{M}\right] \cdot \mathbf{X} = \mathbf{F}, \tag{3}$$

which is a block diagonal matrix with blocks proportional to K

$$\mathbf{C} = \begin{bmatrix} \delta_1 \cdot K & 0 & \cdots & \cdots & 0 \\ 0 & \delta_2 \cdot K & \ddots & & \vdots \\ \vdots & \ddots & \ddots & \ddots & \vdots \\ \vdots & & \ddots & \ddots & 0 \\ 0 & \cdots & \cdots & 0 & \delta_N \cdot K \end{bmatrix}. \tag{4}$$

Note that, as a first approximation, only linear in-sector damping is considered in our model, and that the mistuning damping distribution is given by the damping coefficients $\delta_j > 0, \quad j = 1, \ldots, N$.

It is important to highlight that the variation of the damping δ_j from sector to sector is of the order of the damping itself. This is a completely different situation with respect to the case of mass/stiffness mistuning where the mistuning is just a small variation around the tuned value.

In order to have a more clear understanding of the effect of the damping nonuniformity it is convenient to transform the system (3) into the basis of the traveling wave natural modes of the tuned system:

$$\left(\begin{bmatrix} \Omega_1^2 - \omega^2 I & \cdots & 0 \\ \vdots & \ddots & \vdots \\ 0 & \cdots & \Omega_N^2 - \omega^2 I \end{bmatrix} + i\Delta \right) \begin{bmatrix} A_1 \\ \vdots \\ A_j \\ \vdots \\ A_N \end{bmatrix} = \begin{bmatrix} 0 \\ \vdots \\ P_r^H \cdot F \\ \vdots \\ 0 \end{bmatrix}, \tag{5}$$

where the complex amplitudes of the tuned TW modes with k nodal diameters are packed in the vector A_k, and the diagonal matrix Ω_k contains their corresponding

natural frequencies,

$$\Omega_k^2 = \begin{bmatrix} \omega_{k1}^2 & & 0 \\ & \ddots & \\ 0 & & \omega_{km}^2 \end{bmatrix}, \quad \text{for} \quad k = 1 \dots N,$$

and m is the number of DOF per sector.

The resulting mistuning correction matrix in the traveling wave basis is then given by:

$$\Delta = \mathbf{P^H} \cdot \mathbf{C} \cdot \mathbf{P}, \tag{6}$$

and $\mathbf{P}$ is the transformation matrix from the basis of traveling waves to the basis of physical displacements,

$$\mathbf{P} = \frac{1}{\sqrt{N}} \begin{bmatrix} P_1 e^{i(2\pi 1/N)1} & \dots & P_N e^{i(2\pi N/N)1} \\ \vdots & & \vdots \\ P_1 e^{i(2\pi 1/N)j} & \dots & P_N e^{i(2\pi N/N)j} \\ \vdots & & \vdots \\ P_1 e^{i(2\pi 1/N)N} & \dots & P_N e^{i(2\pi N/N)N} \end{bmatrix}, \tag{7}$$

where

$$P_k = [Z_{k1}|Z_{k2}|...|Z_{km}], \tag{8}$$

and the vectors $Z_{k1}, \dots, Z_{km}$ are the complex tuned mode shapes of the m TW modes with k nodal diameters and associated frequencies $\omega_{k1}, \dots, \omega_{km}$. Note that the change from the physical displacements to the TW basis involves performing a discrete Fourier transform of the sector to sector distribution of the system response. The resulting discrete Fourier modes are precisely the TW amplitudes $A_1, \dots, A_N$, which are usually referred to as the nodal diameter spectrum. This spectral representation of the displacements has been proved to be very useful for the analysis of the effects of mistuning, see [15].

After inserting the above expression into Eq. (6), the mistuning correction matrix

Δ takes the form

$$\Delta = \begin{bmatrix} \Delta_{11} & \Delta_{12} & \cdots & \Delta_{1N} \\ \Delta_{21} & \Delta_{22} & \cdots & \Delta_{2N} \\ \vdots & \vdots & \ddots & \vdots \\ \Delta_{N1} & \Delta_{N2} & \cdots & \Delta_{NN} \end{bmatrix} \tag{9}$$

where

$$\Delta_{kj} = \sum_{s=1}^{N} \delta_s \cdot \left(P_k^H \cdot K \cdot P_j \right) \cdot e^{i\left(\frac{2\pi(j-k)}{N}\right)s} \tag{10}$$

The structure of the blocks Δ_{kj} can be described more easily if the discrete Fourier transform of sector damping distribution δ_j is used:

$$\delta_j = \sum_{k=1}^{N} \delta_k^F e^{i\left(\frac{2\pi k}{N}\right)j}. \tag{11}$$

Note that, since δ_j is a real distribution, its Fourier coefficients must verify

$$\delta_k^F = \overline{\delta_{-k}^F}, \tag{12}$$

and the sector averaged damping δ_m is given by

$$\delta_m = \frac{1}{N} \sum_{j=1}^{N} \delta_j = \delta_N^F \tag{13}$$

If we take the Fourier expression for the damping distribution (11) into Eq. (10), the blocks of the mistuning matrix Δ can be finally written as

$$\Delta_{kj} = \delta_{k-j}^F \cdot \left(P_k^H \cdot K \cdot P_j \right). \tag{14}$$

From the above equation it can be concluded that the effect of the mistuning is to couple the natural TW modes; in the absence of damping mistuning the matrix Δ is diagonal and, see Eq. (5), the TW are uncoupled. It is precisely the harmonic $k - j$ of the damping mistuning distribution the one responsible for the coupling of the TW with k and j nodal diameters. This coupling effect means that, unlike what happens in the tuned case, other TW modes different from the TW directly forced

(i.e., the TW with number of nodal diameter equals to the engine order r) appear in the forced response of the mistuned bladed disk.

Asymptotic derivation of the AMM

No simplifying approximations have been performed in the previous section. The full FEM equations of motion for the forced response of the mistuned bladed disk, Eq. (3) have just been written in the tuned TW basis, and the damping mistuning contribution has been expressed in terms of the Fourier modes of the sector-to-sector damping distribution, see Eqs. (5), (9) and (14).

In this section, an asymptotic procedure is applied to obtain the simplified AMM from Eq. (5). Similar AMM derivations for the effect of elastic (mass/stiffness) mistuning can be found in the references [11] and [12], for the cases of flutter and forced response, respectively.

In order to see which TW modes are more relevant, we now make use of the fact that the damping δ_j is small, which means that, in the unforced problem, it induces a temporal decay of the response that takes place in a time scale much slower than the oscillation period.

The AMM is derived retaining only the dominant terms in Eq. (5) and neglecting the terms that produce a small correction. Note that, to have a maximum tuned response amplitude normalized to 1, the forcing term in the right hand side of Eq. (5) has to be of size δ_m and, therefore, it is also a small term.

The forcing has engine order r, and when the forcing frequency ω is close to resonant tuned frequency ω_0 (corresponding to a TW with r nodal diameters), two types of TW modes can be distinguished:

1. Passive modes that, in first approximation, do not have any effect on the forced response amplitude. These modes have frequencies ω_{kj} that are not close to the resonant frequency ω_0, in other words, for the passive modes $|\omega_{kj} - \omega_0|$ is large as compared with the damping terms. Note that the subindex $k = 1 \dots N$ and $j = 1 \dots m$ represent respectively the nodal diameter and corresponding mode shapes. The equations for these modes in the system (5) are of the form:

$$(\omega_{kj}^2 - \omega^2) A_{kj} = \sum_{i,h=1}^{N,m} (\text{small damping terms}) A_{ih} + (\text{small forcing}) \qquad (15)$$

Since we are forcing near resonance, ω is close to ω_0, and then $|\omega_{kj} - \omega| \sim |\omega_{kj} - \omega_0|$ and the coefficient in left hand side of the equation is large as compared to the damping and forcing terms. Consequently, the right hand side of the above equation can be neglected, and gives, in first order approximation:

$$A_{kj} \simeq 0 \tag{16}$$

2. Active modes that take part in the forced response. These modes have frequencies ω_a close to the resonant frequency ω_0. Their equation from the system (5) can be written as:

$$(\omega_a^2 - \omega^2)A_a + i \sum \delta_{aa'} A_{a'} = F_a \tag{17}$$

with

$$\delta_{aa'} = \delta^F_{a-a'}(Z_a^H K Z_{a'}) \tag{18}$$

where Z_a, $Z_{a'}$, a and a' are, respectively, the indexes of the active modes A_a and $A_{a'}$, ω_a is the frequency of the active mode, and the forcing F_a is equal to zero for all the modes with nodal diameter different from the engine order r.

Once the passive modes have been removed from Eq. (5), the equations for the active modes can be expressed as

$$\begin{bmatrix} d_k & & & \cdots & \\ & d_{k+1} & & i \cdot D & \\ & \ddots & \ddots & \ddots & \vdots \\ \vdots & i \cdot D^H & \ddots & d_{-(k+1)} & \vdots \\ & & \cdots & & d_{-k} \end{bmatrix} \begin{bmatrix} A_k \\ A_{k+1} \\ \vdots \\ A_{-(k+1)} \\ A_{-k} \end{bmatrix} = \begin{bmatrix} 0 \\ \vdots \\ i \cdot \delta_m \cdot f_r \\ \vdots \\ 0 \end{bmatrix}. \tag{19}$$

which is the AMM formulation for the active TWs: $A_k, A_{k+1}, ..., A_{-k}$. The forcing coefficient f_r is set to

$$f_r = (Z_r^H K Z_r) \tag{20}$$

in order to have tuned maximum response 1. The diagonal terms are given by

$$d_k = (\omega_k^2 - \omega^2) + i\delta_m(Z_k^H K Z_k) \tag{21}$$

and the off-diagonal elements D are of the form

$$D_{kk'} = \delta^F_{k-k'}(Z_k^H K Z_{k'}). \tag{22}$$

The resulting AMM written in Eq. (19) reduces drastically the size of the problem (5) to the number of active modes. The AMM retains only the minimal set of TW that take part in the forced response of the mistuned system (the active TW modes). The rest of the modes (the passive TW modes) have frequencies that are far away from the frequency of the directly forced mode and, in first approximation, are not excited by the forcing and can be neglected. The derivation of the AMM requires to know only the tuned vibration characteristics of the system and the damping distribution, and it gives precise information on which Fourier harmonics of the damping distribution induce a coupling between the active TW modes.

Frequency shift due to damping mistuning

The absence of frequency shift in the forced response of a rotor with damping mistuning can be proved analytically using the AMM formulation.

The mistuned natural vibration characteristics of the system can be obtained from the same AMM system in Eq. (19) just by setting the forcing to zero and solving the resulting eigenvalue problem for ω. Note that now ω is a complex number; its real part is the mistuned natural vibration frequency and its imaginary part is the damping.

If the AMM matrix is premultiplied by the row vector

$$\overline{[A_k, A_{k+1}, \ldots, A_{-(k+1)}, A_{-k}]}$$

(the over-bar means complex conjugation), and the real part is taken, then the following expression is obtained:

$$\sum_{j=-k}^{k} |A_j|^2(\omega_j^2 - \Re(\omega^2)) = 0, \tag{23}$$

where $\Re$ stands for the real part.

The natural vibration frequencies of all active TW modes ω_j, and the eigenvalue ω are both very close to the frequency of the cluster of modes ω_0, and, therefore,

they can be written as

$$\omega_j = \omega_0(1 + \Delta\omega_j),$$
$$\omega = \omega_0(1 + \Delta\omega),$$

with $|\Delta\omega_j| \ll 1$ and $|\Delta\omega| \ll 1$. If these expansions are taken to Eq. (23), and the higher corrections in $\Delta\omega_j$ and $\Delta\omega$ are neglected, then it simplifies to

$$\sum_{j=-k}^{k} |A_j|^2(\Delta\omega_j - \Re(\Delta\omega)) = 0. \tag{24}$$

In the expression above $|A_j|^2 \geq 0$, and, since the sum has to be 0, $\Re(\Delta\omega)$ cannot be above or below all the $\Delta\omega_j$, it has to be in between them, that is,

$$\min_{j=-k\ldots k}(\Delta\omega_j) \leq \Re(\Delta\omega) \leq \max_{j=-k\ldots k}(\Delta\omega_j).$$

The mistuned natural frequencies are in between the frequencies of the clustered tuned active TW modes, which have all very similar values. In other words, it can be concluded that, in contrast to what happens with the mass/stiffness mistuning, there is no appreciable frequency splitting associated with the effect of damping mistuning.

Results and Discussion

The effect of damping mistuning on the forced response of the simple 1-DOF spring-mass model shown in Fig. 3 is analyzed in this section. The spring mass system is given by

$$\ddot{x}_j + \omega_a^2 x_j + \omega_c^2(2x_j - x_{j+1} - x_{j-1}) + c\delta_j \dot{x}_j = f e^{\mathrm{i}(\omega t + 2\pi(r/N)j)} + \text{c.c.}, \quad j = 1 \ldots N, \tag{25}$$

where c.c. means complex conjugate, $N = 50$ sectors, $\omega_a^2 = \omega_c^2 = 1$, δ_j is the mistuning distribution with average value one ($\delta_m = 1$), c is the damping coefficient, and f is scaled in order to have tuned response equal to 1.

The tuned vibration characteristics of the mass-spring system are also represented in Fig. 3, where the two thick black vertical lines indicate the two forcing cases that are going to be considered: (i) forcing with engine order $r = 7$ (isolated modes, IM), and (ii) forcing with engine order $r = 24$ (clustered modes, CM).

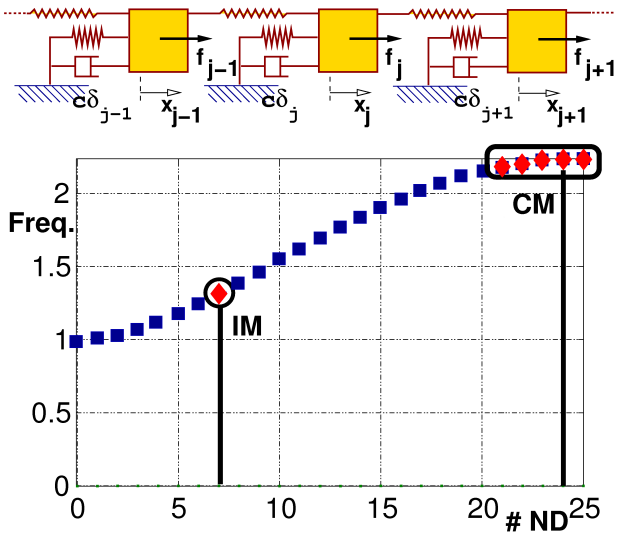

Figure 3: Top: sketch of the simple 1-DOF per sector system. Bottom: tuned frequencies vs. number of nodal diameters (IM: forcing engine order 7, CM: forcing engine order 24).

In order to check the accuracy of the AMM, the mass-spring system response for the two forcing configurations is computed and compared with the AMM predictions.

Forcing of isolated modes

This first case corresponds to forcing the tuned TW mode with 7 nodal diameters and vibration frequency $\omega_0 = 1.3135\ldots$, which is well apart from the rest, i.e., its distance to the frequencies of the remaining TW modes is large as compared with the small damping, see Fig. 3. This is the simplest possible configuration, which corresponds to the forcing of an isolated mode (labeled IM in Fig. 3). The only active modes that are present in the mistuned response are the forced TW and its symmetric one (also with 7 nodal diameters and the same frequency ω_0, but rotating in the opposite direction), and the corresponding AMM description includes only these two active TW modes.

The AMM (see Eq. (19)) for this case consists of only two equations, and takes the form:

$$\begin{bmatrix} (\omega_0^2 - \omega^2) + i\delta_m D_0 & i\delta_{2r}^F D \\ i\overline{\delta_{2r}^F D} & (\omega_0^2 - \omega^2) + i\delta_m D_0 \end{bmatrix} \begin{bmatrix} A_{+r} \\ A_{-r} \end{bmatrix} = \begin{bmatrix} i\delta_m D_0 \\ 0 \end{bmatrix} \tag{26}$$

where:

$$D_0 = Z_{+r}^H K Z_{+r} \quad \text{and} \quad D = Z_{+r}^H K Z_{-r}, \tag{27}$$

and the response of the system consists of the superposition of the two TW modes with amplitudes $A_{\pm r}$

$$X_j = (Z_{+r} A_{+r} \mathrm{e}^{\mathrm{i}(2\pi r/N)j} + Z_{-r} A_{-r} \mathrm{e}^{-\mathrm{i}(2\pi r/N)j}), \quad \text{for } j = 1, \ldots, N. \tag{28}$$

Note that, from the above system, it can be concluded right away that only the harmonic $2r = 14$ of the damping mistuning distribution has a noticeable effect on the vibratory response of the system.

If the rescaled frequency

$$\Delta\omega = \frac{\omega_0^2 - \omega^2}{\delta_m D_0}, \tag{29}$$

and rescaled damping mistuning

$$d\mathrm{e}^{\mathrm{i}\phi} = \frac{\delta_{2r}^F}{\delta_m}\frac{D}{D_0}, \tag{30}$$

are used, then the AMM further simplifies to

$$\begin{bmatrix} \Delta\omega + i & id\mathrm{e}^{\mathrm{i}\phi} \\ id\mathrm{e}^{-\mathrm{i}\phi} & \Delta\omega + i \end{bmatrix} \begin{bmatrix} A_+ \\ A_- \end{bmatrix} = \begin{bmatrix} i \\ 0 \end{bmatrix}, \tag{31}$$

which can be easily solved analytically to give

$$A_{+r} = \frac{i[\Delta\omega + i]}{[\Delta\omega + i]^2 + d^2},$$
$$A_{-r} = \frac{de^{-i\phi}}{[\Delta\omega + i]^2 + d^2}.$$

The vibration amplitude of blade $j = N$ can be written as

$$\text{Amplitude} \propto |A_{+r} + A_{-r}|, \tag{32}$$

and, using the solution of the AMM, the amplification factor due to damping mistuning can be finally expressed in closed form as

$$\text{AF} = \frac{\left|[1 - i\Delta\omega] - de^{-i\phi}\right|}{\left|[1 - i\Delta\omega]^2 - d^2\right|}. \tag{33}$$

Note that, for the tuned case $d = 0$, the maximum value of the above AF is 1.

In order to find the maximum amplification due to damping mistuning the expression for the AF (Eq. (33)) is explored as a function of the three parameters: $\Delta\omega$, d, and ϕ. The resulting maximum values of the amplification factor AF (Eq. (33)) over the angle ϕ for any given values of $\Delta\omega$ and d are plotted in the left plot Fig. 4.

In order to avoid the unphysical possibility of having a negative damping, the $2r$ Fourier coefficient of the mistuning damping distribution δ_{2r}^F has to be limited to (see the expressions (11) and (12))

$$|\frac{\delta_{2r}^F}{\delta_m}| < 0.5.$$

On the other hand,

$$\left|\frac{D}{D_0}\right| \leq 1,$$

as it can be readily obtained from Eq. (27) using the fact that $Z_{+r} = \overline{Z_{-r}}$ and K is a real symmetric non-negative matrix, so the size of the scaled damping mistuning is limited to

$$d = |\frac{\delta_{2r}^F}{\delta_m}||\frac{D}{D_0}| < 0.5.$$

and the resulting amplitude factor can be, therefore, as high as $AF = 2$ for this simple case (see the left plot Fig. 4). For any given rescaled mistuning damping amplitude d, the maximum AF is obtained for $\Delta\omega = 0$, that is, for the forcing frequency equal to the frequency of the forced tuned TW. The maximum AF as a function of d has the very simple expression

$$\mathrm{AF}_{max} = \frac{1}{1-d}. \tag{34}$$

which is plotted in the right plot of Fig. 4. The maximum AF increases as d is increased, that is, if the average damping δ_m is kept fixed, the AF increases as the coefficient of the $2r$ Fourier mode of the damping mistuning distribution δ_r is increased.

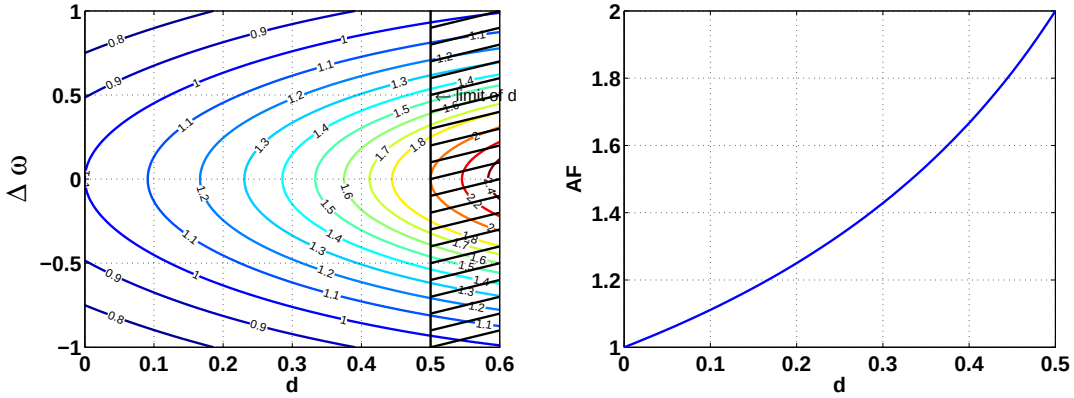

Figure 4: Left: Maximum AF (Eq. (33)) as a function of the mistuning amplitude $d \leq 0.5$ and the frequency $\Delta\omega$. Right: Maximum amplification factor as a function of mistuning amplitude d ($\Delta\omega = 0$).

In order to check the above results, several simulations of the mass-spring system given by Eq. (25) have been performed for engine order forcing $r = 7$, moving the forcing frequency close to that of the isolated mode frequency labeled IM in Fig. 3,

$\omega_0 = 1.3135\ldots$, and with small damping coefficient $c = 0.01/\omega_0$.

The case in Fig. 5 corresponds to computing the forced response of the mass-spring system with a damping mistuning pattern that has only the Fourier mode $2r = 14$, with amplitude $\delta_{14}^F/\delta_m = 0.25$,

$$\delta_j = \delta_m(1 + 0.5\cos(2\pi\frac{14}{N}j)), \quad j = 1\ldots N. \tag{35}$$

The maximum displacement for each sector is computed during the forcing frequency sweep, and the results are plotted with blue lines in the top left plot, where the envelope is also indicated with a thick red line. The obtained maximum amplitude $AF_{max} = 1.332$, is in very good agreement with the AMM prediction $AF_{\text{AMM}} = 1.333$, which is given by Eq. (34) for the particular value of

$$d = |\frac{\delta_{2r}^F}{\delta_m}||\frac{D}{D_0}| = 0.25 \times 1 = 0.25,$$

and is marked with a horizontal black line. The mistuning damping of the different blades is represented in the left middle plot, and, in the bottom plot, the Fourier coefficients of the mistuning damping distribution are shown (only the average mode and the $2r = 14$ mode are present in this case). The resulting amplitude of the different TW modes as the forcing frequency is varied is represented in right plot of Fig. 5. Note that, again in perfect agreement with the AMM predictions, the only TW modes involved in the mistuned response are those with wavenumber 7 and -7.

The forced response of the mass-spring system is now computed for a damping mistuning pattern that is made of the previous pattern with a random variation superimposed.

$$\delta_j = \delta_m(1 + 0.50\cos(2\pi\frac{14}{N}j) + \text{random}_j), \quad j = 1\ldots N. \tag{36}$$

The random component is chosen to have no Fourier harmonic 14, so, for this second damping mistuning pattern $\delta_{14}^F/\delta_m = 0.25$, as in the previous case. The corresponding results are given in Fig. 6. The response of the system is practically the same as in the previous case, with $AF_{max} = 1.338$, despite of the now more complex damping mistuning pattern, which exhibits sectors with much smaller damping values. This, as predicted by the AMM, is due to the fact that the only component of the damping

mistuning pattern that affects the system response is δ_F^{14}, and this one has not been changed.

The third damping mistuning pattern considered is obtained by removing the Fourier harmonic 14 in the previous pattern

$$\delta_j = \delta_m(1 + \text{random}_j), \quad j = 1 \dots N. \tag{37}$$

The forced response of the mass-spring system is shown in Fig. 7, where it can be clearly appreciated that the damping mistuning pattern with $\delta_F^{14} = 0$ has practically no noticeable effect on the system response. The system behaves as if it were tuned, showing no noticeable amplification of the forced response, $AF_{max} = 0.992$, despite of the fact that there is a strong sector to sector variation of the damping, with some sectors showing very small values of the damping. This confirms again the AMM prediction about δ_F^{14} being the sole cause of the amplification of the forced response.

Finally, to once again confirm the AMM predictions, a fourth mistuning distribution is used that contains only the Fourier harmonic $\delta_{19}^F/\delta_m = 0.25$,

$$\delta_j = \delta_m(1 + 0.50\cos(2\pi\frac{19}{N}j)), \quad j = 1 \dots N. \tag{38}$$

The results in Fig. 8 indicate that, with $\delta_{14}^F = 0$, the system behaves again as if there were no mistuning at all present, with an amplification factor of $AF_{max} = 0.998$.

In summary, the damping mistuning effect in the forcing of a TW with tuned frequency well apart from its neighbors (i.e. with a frequency gap large as compared with the damping) can produce an amplification of the forced response amplitude only when the damping distribution contains precisely the Fourier harmonic with wavenumber equal to twice the engine order of the forcing.

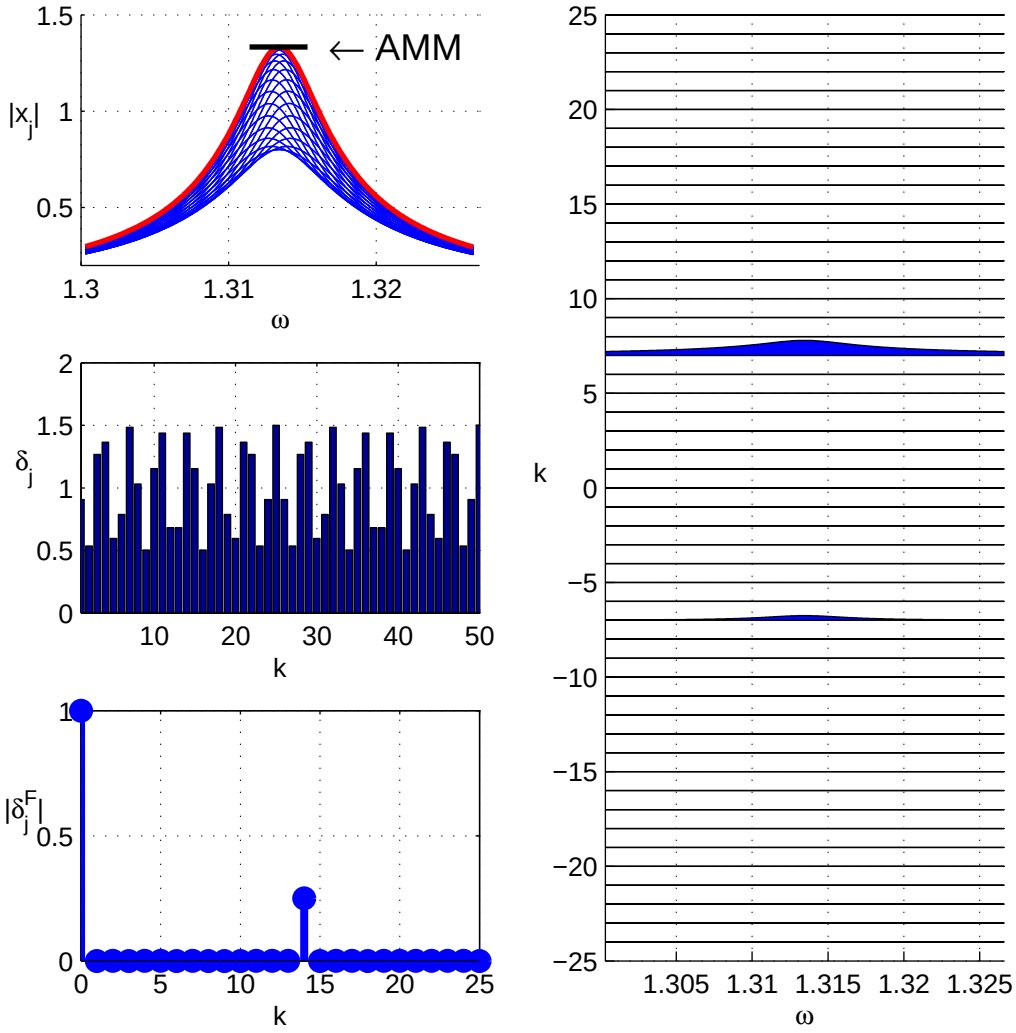

Figure 5: Response of the mistuned mass-spring system in Fig. 3 to a forcing with engine order 7. The damping mistuning pattern is composed of a mean value plus a Fourier mode 14 (see Eq. (35)). Top left: maximum displacements $|x_j|$ vs. forcing frequency (AMM prediction for the maximum value indicated). Middle left: damping mistuning distribution δ_j. Bottom left: amplitude of the Fourier modes of the damping mistuning distribution. Right: amplitude of the TW components of the response vs. forcing frequency (wavenumber in the vertical axis).

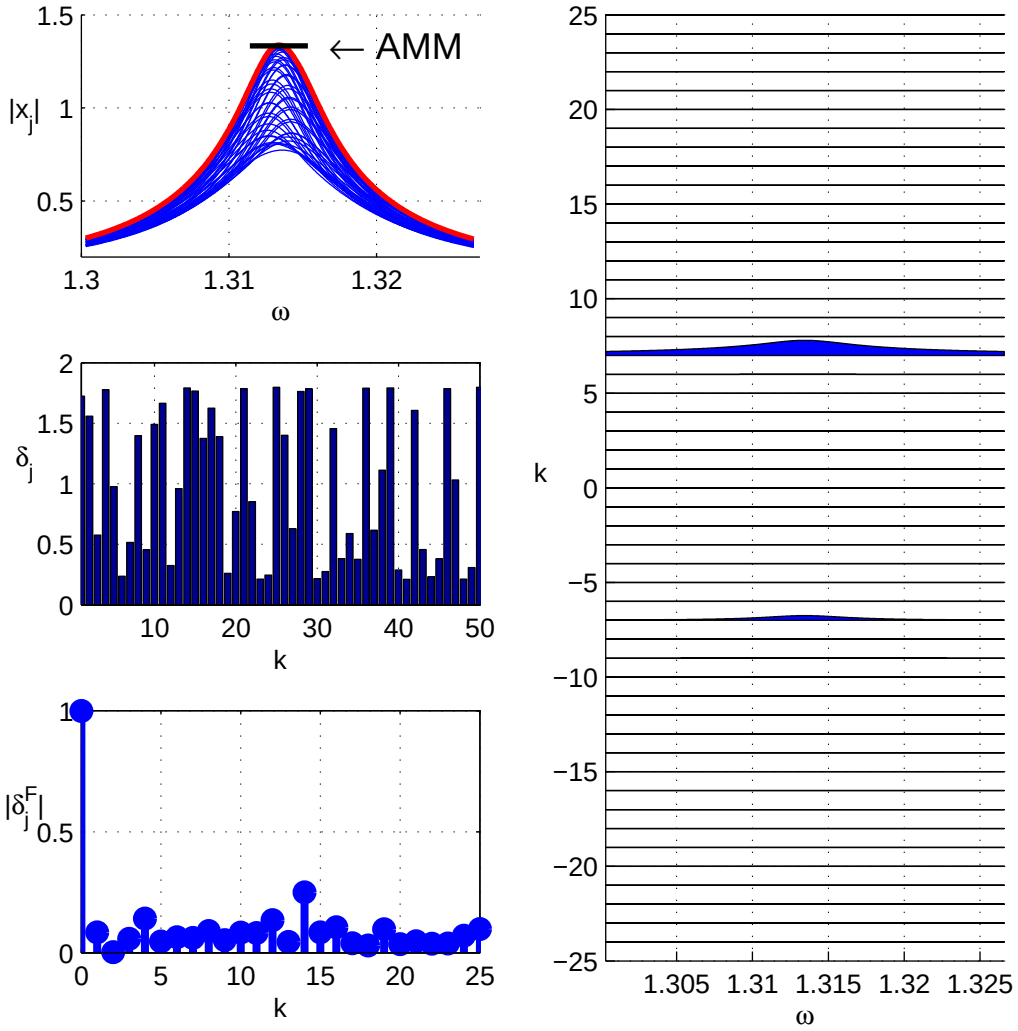

Figure 6: Response of the mistuned mass-spring system in Fig. 3 to a forcing with engine order 7. The damping mistuning pattern is composed of a mean value plus a Fourier mode 14 and a random distribution (see Eq. (36)). Top left: maximum displacements $|x_j|$ vs. forcing frequency (AMM prediction for the maximum value indicated). Middle left: damping mistuning distribution δ_j. Bottom left: amplitude of the Fourier modes of the damping mistuning distribution. Right: amplitude of the TW components of the response vs. forcing frequency (wavenumber in the vertical axis).

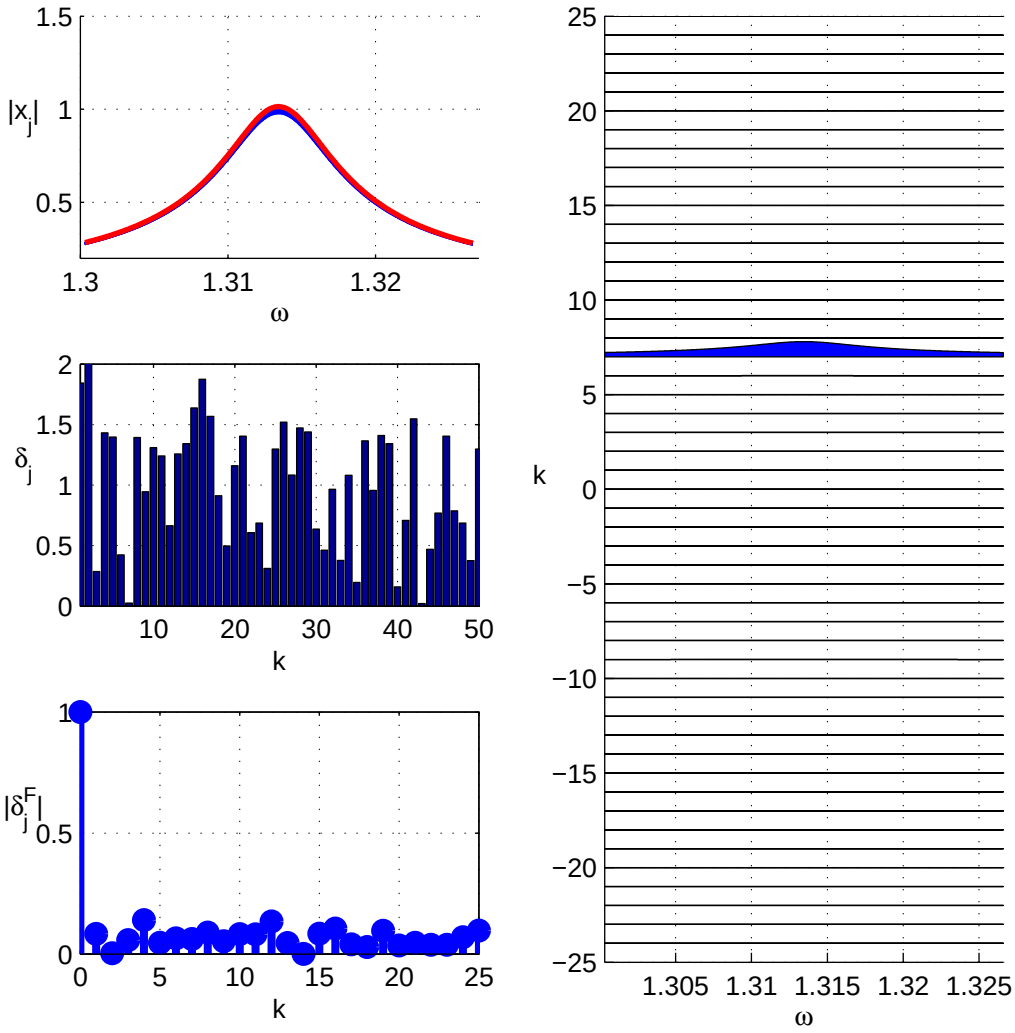

Figure 7: Response of the mistuned mass-spring system in Fig. 3 to a forcing with engine order 7. The damping mistuning pattern is composed of a mean value and a random distribution with zero Fourier mode $2r = 14$ (see Eq. (42)). Top left: maximum displacements $|x_j|$ vs. forcing frequency. Middle left: damping mistuning distribution δ_j. Bottom left: amplitude of the Fourier modes of the damping mistuning distribution. Right: amplitude of the TW components of the response vs. forcing frequency (wavenumber in the vertical axis).

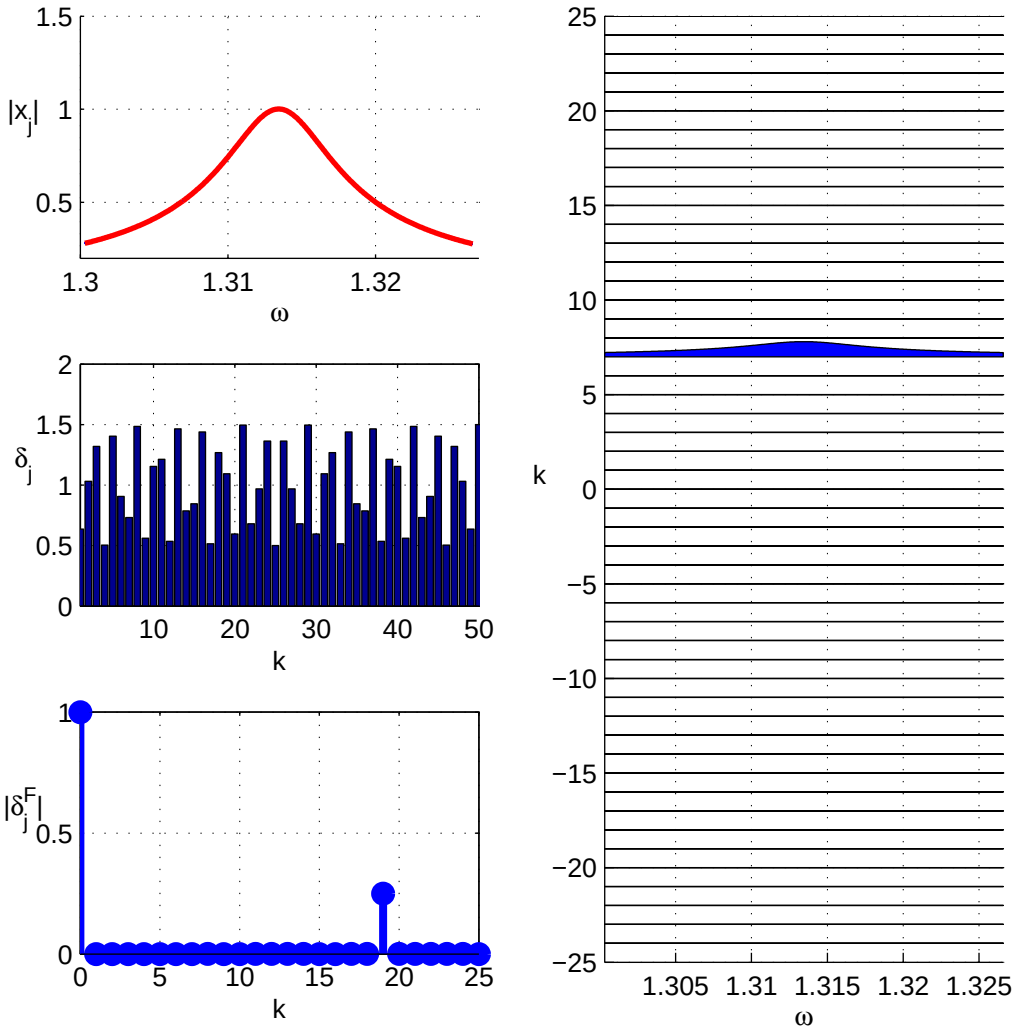

Figure 8: Response of the mistuned mass-spring system in Fig. 3 to a forcing with engine order 7. The damping mistuning pattern is composed of a mean value plus a Fourier mode 19 (see Eq. (42)). Top left: maximum displacements $|x_j|$ vs. forcing frequency. Middle left: damping mistuning distribution δ_j. Bottom left: amplitude of the Fourier modes of the damping mistuning distribution. Right: amplitude of the TW components of the response vs. forcing frequency (wavenumber in the vertical axis).

Forcing of clustered modes

The mass-spring system is forced with an engine order $r = 24$, near the resonant tuned TW, which has frequency $\omega_0 = 2.1830$, and with a small damping coefficient $c = 0.03/\omega_0$. The forced TW is on the horizontal part of the frequency distribution of the modal family (see the encircled modes labeled CM in Fig. 1), and, therefore, there are more active TW modes (those with frequency close to ω_0) in this case: those with nodal diameters $21, 22, 23, 24, 25$, and the symmetric ones $-24, -23, -22, -21$.

The AMM description, according to Eq. (19), can now be written as 9×9 linear system

$$\begin{bmatrix} d_{21} & & & & & \\ & d_{22} & & & iD & \\ & & \ddots & & & \\ & & & d_{-22} & & \\ & iD^{\mathrm{H}} & & & & \\ & & & & & d_{-21} \end{bmatrix} \begin{bmatrix} A_{21} \\ A_{22} \\ \vdots \\ A_{-22} \\ A_{-21} \end{bmatrix} = \begin{bmatrix} 0 \\ \vdots \\ \mathrm{i}\delta_m f_r \\ \vdots \\ 0 \end{bmatrix}, \tag{39}$$

for the amplitudes of the 9 active TW modes:

$$A_{21}, A_{22}, A_{23}, A_{24}, A_{25}, A_{-24}, A_{-23}, A_{-22}, A_{21}.$$

The damping mistuning harmonics that appear in the off-diagonal terms of the AMM matrix are

$$\delta_1^F, \delta_2^F, \ldots, \delta_8^F,$$

which are the only that effectively couple the 9 active TWs $A_{21}, \ldots, A_{-21}$, and the vibration amplitude of blade $j = N$ can be written as

$$\text{Amplitude} \propto |A_{21} + A_{22} + \cdots + A_{-22} + A_{-21}|, \tag{40}$$

The AMM indicates that only the damping mistuning harmonics with wavenumber from 1 to 8 actually have effect on the response of the system. In order to check this prediction, the following mistuning pattern is used

$$\delta_j = \delta_m(1 + 0.2\cos(2\pi\frac{1}{N}j) + 0.2\cos(2\pi\frac{3}{N}j) + 0.5\cos(2\pi\frac{8}{N}j)), \quad j = 1 \ldots N, \tag{41}$$

which contains only the Fourier harmonics 1, 3, and 8. The response of the mass-

spring system gives a maximum amplification factor $AF_{max} = 1.382$, much larger than the tuned one, see Fig. 9. On the other hand, the results shown in Fig. 10 correspond to a damping mistuning pattern with harmonics with wavenumber 13, 16 and 20

$$\delta_j = \delta_m(1 + 0.2\cos(2\pi\frac{13}{N}j) + 0.2\cos(2\pi\frac{16}{N}j) + 0.5\cos(2\pi\frac{20}{N}j)), \quad j = 1\ldots N, \quad (42)$$

all of them not active according to AMM, and, in this case, there is no detectable effect of the mistuning and no amplification of the response of the system ($AF_{max} = 1.004$), even though there are in-sector damping values as small as 0.25.

The resulting AMM is again much simpler than the original problem, but it is still too complicated to obtain an explicit expression for the maximum amplification factor as it was done in the previous section. So, in this case, the damping mistuning distribution that leads to the maximum amplification factor is located using an optimization algorithm. The optimization is performed for both, the mass-spring system and the AMM approximation, and the results are compared to quantitatively check the validity of the AMM calculations.

The applied optimization process looks for the damping mistuning distribution $\delta_1, \ldots, \delta_N$ that maximizes the forced response of the system. The average damping is fixed δ_m, and the sector damping values are allowed to vary in the range $\delta_j/\delta_m \in [0.5, 1.5], \quad j = 1, \ldots, N$. For each excitation frequency ω the optimization generates a maximum response and the corresponding damping mistuning distribution, and the frequency ω is varied in the vicinity of the resonant frequency ω_0 to locate the global maximum response.

The forced response of the system with the damping distribution that gives global maximum amplitude is then computed performing a frequency sweep around the resonant frequency ω_0. The results are presented in Fig. 11 and Fig. 12, for, respectively, the mass-spring system model and the AMM approximation. The resulting maximum amplification factors are very similar: $AF_{max} = 1.6514$ for the mass-spring system, and $AF_{max} = 1.6321$ for the AMM. And the damping mistuning pattern that gives the maximum AF is practically identical for the two cases, except for a shift of 8 sectors. It is interesting to notice that the most important Fourier mode of the damping distribution is now δ_1^F. This Fourier mode produces a coupling of the directly forced TW ($k = 24$) with its adjacent TW modes, which now are also

active modes. The result is that the TWs that have some appreciable magnitude are only those active TW modes around the directly forced TW ($k = 24$), as it can be clearly seen in the right plot of both Fig. 11 and Fig. 12.

As a last check of the AMM predictions, a simulation of the forcing of the mass-spring system is performed for a mistuning distribution that is equal to the one that gives maximum AF (see Fig. 11) but with the Fourier harmonics from 1 to 8 removed. These are precisely the Fourier harmonics of the mistuning distribution that, according to the AMM, have an effect on the forced response of the system. It is clearly seen in Fig. 13 that, without these Fourier harmonics in the damping mistuning distribution, the system falls back to the tuned dynamics.

In summary, the AMM quantitatively predicts the forced response of the mistuned mass-spring system. Even in the case of clustered modes, where several active TW modes have to be kept in the AMM formulation, the size of the AMM is always much smaller than that of the complete system, and, therefore, using the AMM the computation of the mistuned forced response and its optimization is dramatically faster and requires much less CPU cost.

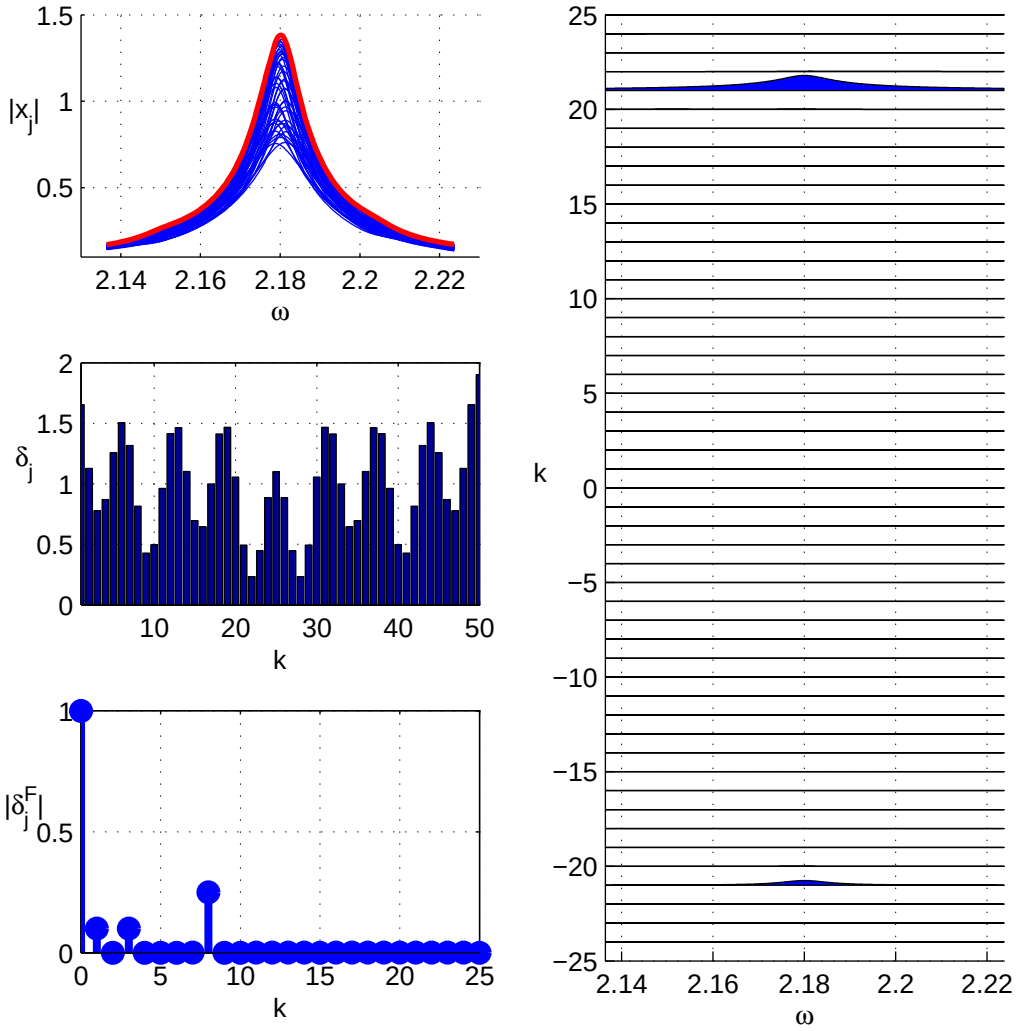

Figure 9: Response of the mistuned mass-spring system in Fig. 3 to a forcing with engine order 24. The damping mistuning pattern is composed of a mean value plus the Fourier modes 1, 3 and 8 (see Eq. (41)). Top left: maximum displacements $|x_j|$ vs. forcing frequency. Middle left: damping mistuning distribution δ_j. Bottom left: amplitude of the Fourier modes of the damping mistuning distribution. Right: amplitude of the TW components of the response vs. forcing frequency (wavenumber in the vertical axis).

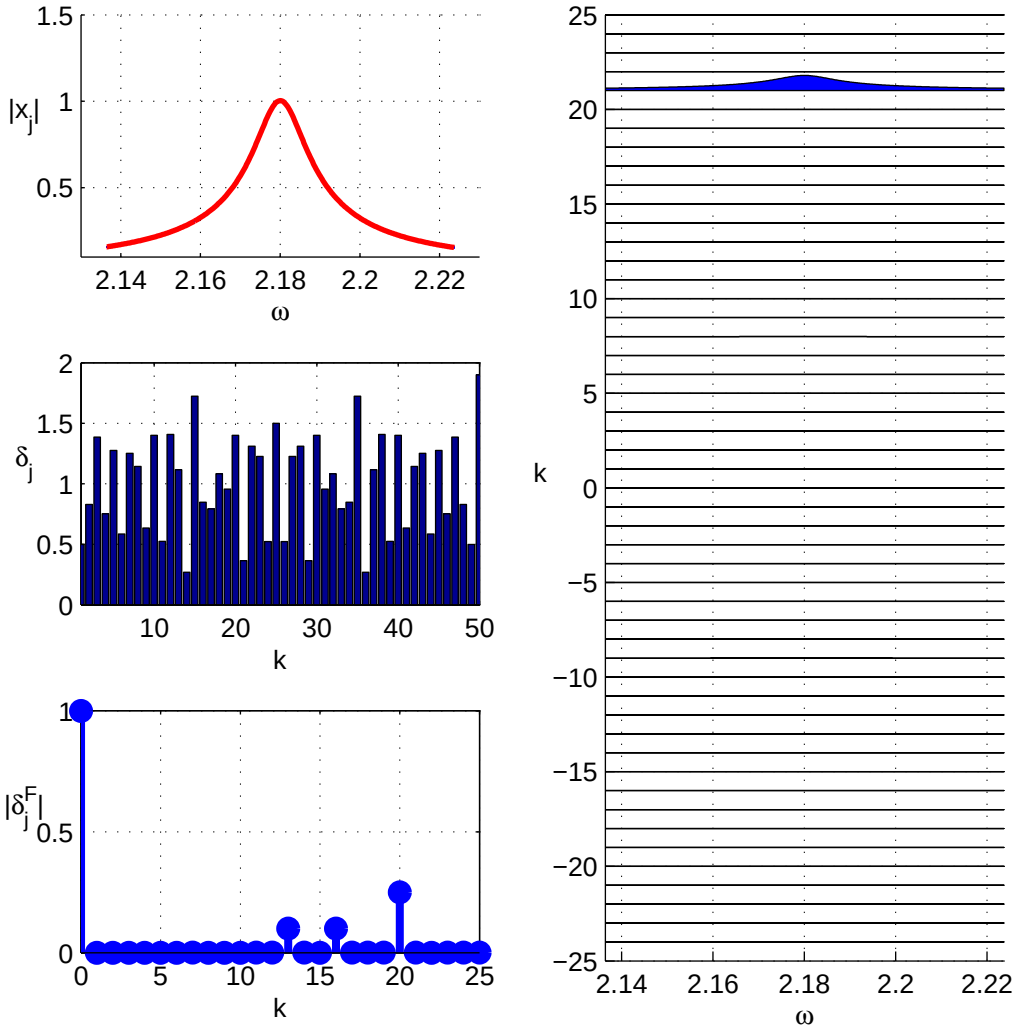

Figure 10: Response of the mistuned mass-spring system in Fig. 3 to a forcing with engine order 24. The damping mistuning pattern is composed of a mean value plus the Fourier modes 13, 16 and 20 (see Eq. (42)). Top left: maximum displacements $|x_j|$ vs. forcing frequency. Middle left: damping mistuning distribution δ_j. Bottom left: amplitude of the Fourier modes of the damping mistuning distribution. Right: amplitude of the TW components of the response vs. forcing frequency (wavenumber in the vertical axis).

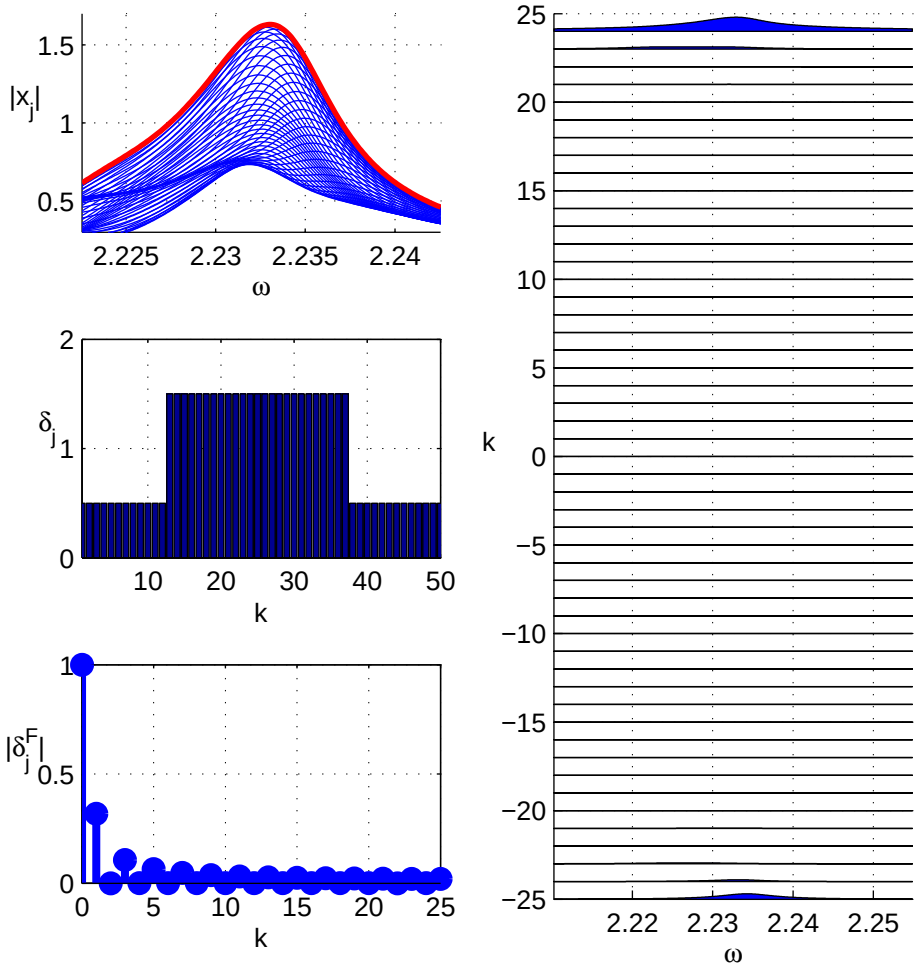

Figure 11: Response of the mistuned mass-spring system in Fig. 3 to a forcing with engine order 24. The mistuning pattern has been optimized to give maximum response amplitude. Top left: maximum displacements $|x_j|$ vs. forcing frequency. Middle left: damping mistuning distribution δ_j. Bottom left: amplitude of the Fourier modes of the damping mistuning distribution. Right: amplitude of the TW components of the response vs. forcing frequency (wavenumber in the vertical axis).

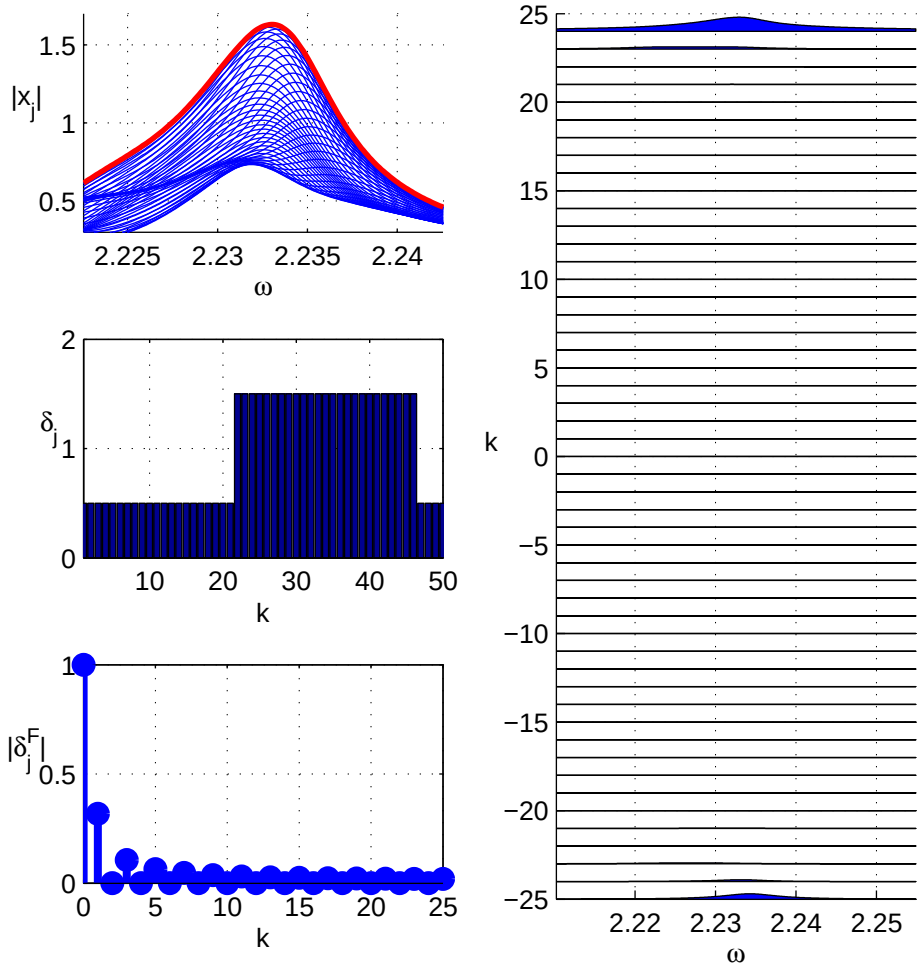

Figure 12: Response of the mistuned mass-spring system in Fig. 3 to a forcing with engine order 24 computed using the AMM. The mistuning pattern has been optimized to give maximum response amplitude. Top left: maximum displacements $|x_j|$ vs. forcing frequency. Middle left: damping mistuning distribution δ_j. Bottom left: amplitude of the Fourier modes of the damping mistuning distribution. Right: amplitude of the TW components of the response vs. forcing frequency (wavenumber in the vertical axis).

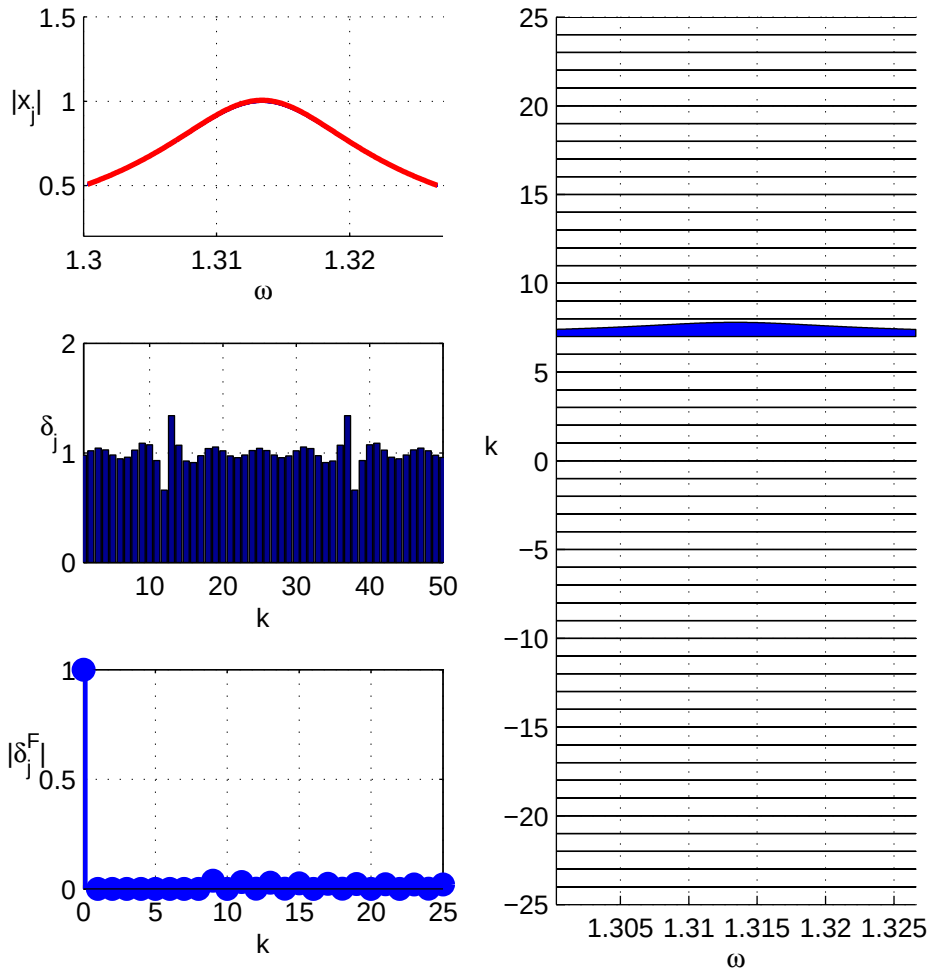

Figure 13: Response of the mistuned mass-spring system in Fig. 3 to a forcing with engine order 24. The mistuning pattern is the optimal one in Fig. 11 but with all Fourier modes from 1 to 8 removed. Top left: maximum displacements $|x_j|$ vs. forcing frequency. Middle left: damping mistuning distribution δ_j. Bottom left: amplitude of the Fourier modes of the damping mistuning distribution. Right: amplitude of the TW components of the response vs. forcing frequency (wavenumber in the vertical axis).

Conclusions

The AMM (Asymptotic Mistuning Model) has been used to analyze the effect of damping mistuning on the forced response of a bladed disk. We analyze the case of linear damping, with a mistuning sector to sector variation of the damping that is of the order of the mean damping itself (i.e., it is not a small modulation over the tuned value).

The AMM is systematically derived from the general equations for the forced response of a mistuned bladed disk using an asymptotic expansion procedure that is based solely on the smallness of the damping (as compared with the forcing frequency), and it retains only the tuned TW modes of the complete rotor that have a natural frequency close to that of the directly forced TW.

The AMM has been applied to compute the effect of damping mistuning in two frequent situations: forced response of a pair of isolated modes, and forced response of a group of modes with close frequencies.

The results from the AMM have been successfully compared with those from a simple 1 DOF per sector mass-spring system. The AMM not only produces quantitatively accurate results using a extremely reduced model; it also gives information on the mechanisms of action of the damping mistuning pattern on the forced response of the system.

The application of the AMM allows us to draw the following final remarks about the effect of damping mistuning:

1. Damping mistuning can increase the forced response of the system. The harmonics of the damping mistuning distribution that couple active TW modes can induce an increase of the forced response, but the rest of the harmonics do not produce any appreciable effect on the system response. In other words, the system has zero sensibility (in first approximation) to the harmonics of the damping mistuning pattern that do not couple active TW modes

2. The presence of small in-sector values of the damping does not necessarily implies an amplification of the forced response (see Fig. 7). This is because the relevant damping values are certain Fourier coefficients of the damping distribution, and not the particular damping value of a sector.

3. From Fig. 4 it can be clearly appreciated that the amplification factor grows monotonously with the amplitude of the damping mistuning. This rules out the possibility of using intentional damping mistuning as a way to reduce the amplification factor.

4. Lin and Mignolet concluded in [5] that damping mistuning can lead to a severe increase in the forced response amplitude, which can be larger than that resulting from mass/stiffness mistuning. This is in agreement with our results: in the case of isolated modes, the maximum amplification due to damping mistuning is $AF_{max} = 2$ (see Fig. 4), while for mass/stiffness mistuning the maximum amplification is always lower than $AF_{max} = (1 + \sqrt{2})/2 = 1.207\ldots$ [12]. If there are more active TW involved in the mistuned response of the system the maximum amplification factor can be even higher (see Fig. 11).

5. And finally, it is interesting to highlight that, as opposed to what happens with the mass/stiffness mistuning, the damping mistuning amplification of the forced response does not produce any appreciable frequency splitting (as it can be seen in figures Fig. 5 to Fig. 12 of this report, and in [6]). This is an important characteristic of damping mistuning that can be used to identify its presence from experimental measurements.

References

[1] J.C. Slater, R.G. Minkiewicz, and A.J. Blair. Forced response of bladed disk assemblies - a survey. *The Shock and Vibration Digest*, 31:17–24, 1999.

[2] M.P. Castanier and C. Pierre. Modeling and analysis of mistuned bladed disk status and emerging directions. *Journal of Propulsion and Power*, 22(2):384–396, 2006.

[3] D.J. Ewins. The mistuned blade vibration problem re-visited. *Twelfth International Symposium on Unsteady Aerodynamics, Aeroacoustics and Aeroelasticity of Turbomachines*, October 2009.

[4] D. Hemberger, D. Filsinger, and H.-J. Bauer. Investigations on maximum amplitude amplification factor of real mistuned bladed structures. *presented at the ASME Turbo Expo, Copenhauen, Denmark, 2012, GT2012-68084*, 2012.

[5] C.C. Lin and M.P. Mignolet. Effects of damping and damping mistuning on the forced response vibrations of bladed disks. *Journal of Sound and Vibration*, 193:525–543, 1996.

[6] C. Siewert and H. Stuer. Forced response analysis of mistuned turbine bladings. *presented at the International Gas Turbine Institute Turbo Expo, Glasgow, UK, ASME Paper GT2010-23782*, 2010.

[7] A.G.S. Joshi and B.I. Epurenau. Reduced order models for blade-to-blade damping variability in mistuned blisks. *presented at the ASME Turbo Expo, Vancouver, Canada, 2011, GT2011-45611*, 2011.

[8] D.M. Feiner and J.H. Griffin. A fundamental model of mistuning for a single family of modes. *Journal of Turbomachinery*, 124:597–605, October 2002.

[9] D.M. Feiner and J.H. Griffin. Mistuning identification of bladed disks using fundamental mistuning model–part i: Theory. *Journal of Turbomachinery*, 126:150–158, January 2004.

[10] D.M. Feiner and J.H. Griffin. Misuning identification of bladed disks using fundamental mistuning model–part ii: Application. *Journal of Turbomachinery*, 126:159–165, January 2004.

[11] C. Martel, R. Corral, and J.M. Llorens. Stability increase of aerodynamically unstable rotors using intentional mistuning. *Journal of Turbomachinery*, 130:011005, January 2008.

[12] C. Martel and R. Corral. Asymptotic description of maximum mistuning amplification of bladed disk forced response. *Journal of Engineering for Gas Turbines and Power*, 131:022506, March 2009.

[13] O. Khemiri, C. Martel, and R. Corral. Quantitative validation of the asymptotic mistuned model (amm) using a high fidelity bladed disk model. *presented at the International Gas Turbine Institute Turbo Expo, Glasgow, UK, ASME Paper GT2010-22498*, 2010.

[14] O. Khemiri, C. Martel, and R. Corral. Amm analysis of mistuning effects on bladed disk forced response. *Twelfth International Symposium on Unsteady Aerodynamics, Aeroacoustics and Aeroelasticity of Turbomachines*, October 2009.

[15] J. Yao, J. Wang, and Q. Li. Improved modal localization and excitation factors for understanding mistuned bladed disk response. *Journal of Propulsion and Power*, 27.

List of Symbols, Abbreviations, and Acronyms

δ_m	Sector averaged damping
δ_j, δ_k^F	Damping amplitude at sector j, k Fourier mode of the damping distribution
Δ_{kj}	Damping mistuing block matrix
ω	Frequency of the forcing
ω_0	Tuned natural frequency of the excited TW
ω_a	Active mode tuned natural frequency
A_j	Traveling wave mode amplitude
D, D_{ij}	Mistuning coefficients in the TW basis
F	In-sector forcing vector
f_r	Forcing coefficient
K	In-sector stiffness matrix
K_c	Sector-to-sector coupling stiffness matrix
M	In-sector mass matrix
m	Number of DOF per sector
M_c	Sector-to-sector coupling mass matrix
N	Number of sectors
X_j	In-sector displacement vector
Z_{kj}	Traveling wave in-sector mode shape
$\mathbf{\Delta}$	Damping mistuning matrix in the TW basis
$\mathbf{C}$	Damping matrix
$\mathbf{F}$	External force
$\mathbf{K}$	Stiffness matrix
$\mathbf{M}$	Mass matrix
$\mathbf{P}$	Matrix of change from TW to displacements
$\mathbf{X}$	Independent DOF displacement vector
AF	Amplification factor
AMM	Asymptotic Mistuning Model
d	Mistuning damping amplitude
r	Engine order of the forcing
TW	Traveling wave